# Impact on the Performance and Heat Flow of a Pulse Tube Cooler Miniaturization

**D. Dherbecourt[1], T. Romand[1], L. Marelli[2], J. André[2] and J.M. Duval[1]**

[1]Univ. Grenoble Alpes, CEA, IRIG, DSBT, F-38000 Grenoble, France
[2]CNES, F-31401 Toulouse, France

## ABSTRACT

A pulse tube cooler cooling below 10 K would allow the use of sensitive terahertz detectors for astrophysics and earth observation. It could also simplify the cryogenic subkelvin chains if 4 K cooling is performed. Such coolers have been previously prototyped and tested [1], but needed too much pre-cooling power to be compatible with space applications.

In order to achieve low temperatures when decreasing the heat flow, two pulse tube prototypes have been designed and tested at CEA-DSBT, in collaboration with the French Spatial Agency (CNES). Both are coaxial, twice intercepted at two pre-cooling temperatures, and have the same length. The impact of pulse tube section miniaturizing is measured and analyzed. Interesting results have been observed which shows a decrease in both the lower temperature and the heat flow at intercepts when reducing the pulse tube sections. An analysis of such behavior is proposed.

Considering typical values of pre-cooling of 1 W at 35 K and 3 W at 100 K [2] from a two-stage pulse tube, these coolers could be combined to achieve 9 K. This first proof of concept is validated; next steps are planned to optimize the whole geometry—and not only the sections—and study the regenerator composition in order to gain performance when keeping a reasonable heat flow at intercepts.

## INTRODUCTION

This work aims to eventually achieve a space-qualified pulse tube type cooler working under 10 K, which could allow the use of terahertz type detectors or simplify the sub kelvin cryogenic chains used for Earth observation or astrophysics.

The use of heat intercepts to reach the lowest temperatures on pulse tube coolers is well known, for example to achieve historically around 20 K ([3], [4]). More recently, a temperature under 4 K, and 25 mW at 5 K, were obtained with a one-stage pulse tube intercepted at 20 K [5]. But this system needed precooling of around 8 W at 20 K, which is not compatible with a typically space qualified precooler.

To go further, studies have been made with one-stage pulse tubes with one more intercept, as shown in Figure 1. The presence of this second intercept, in addition to offering another possible available temperature for instruments, splits the precooling heat load on two points. In this con-figuration, our team succeeded in reaching an ultimate temperature of 6.5 K and a cooling power of more than 650 mW at 15 K [6]. However, heat flows at the intercepts were still 4 W on the first stage and 1.4 W on the second stage. In the same configuration, another pulse tube offers above 400 mW

*Cryocoolers 22,* edited by R.G. Ross, Jr., J.R. Raab and S.D. Miller

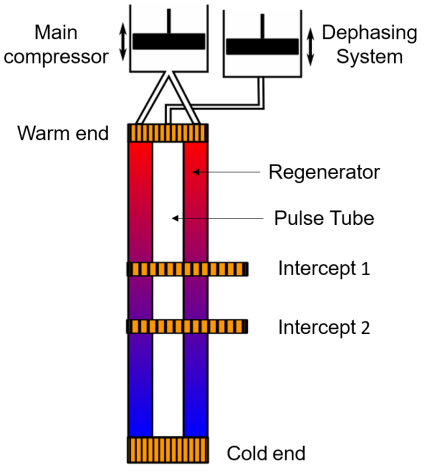


**Figure 1.** Chosen design: a one-stage coaxial pulse tube, twice intercepted

at 15K of cooling power, with 300 W of electrical input power [7]. To achieve this performance, 3.5 W of cold power at the first intercept and 2 W at the second were necessary.

Compared to typical values of pre-cooling of 3 W @ 100 K and 1 W @ 35 K provided by a two-stage cold finger [2], it appears that the heat flow at interfaces need to be decreased in order to optimize the pulse tubes combination.

With this purpose, we chose to play on the geometry of a pulse tube, based on a coaxial one-stage design with two intercepts as described in Figure 1. The performance, heat flows at intercepts, pressure drop and parasitic heat loads are measured and compared between a reference pulse tube and a miniaturized one, where sections are reduced by 45%.

## MATERIAL AND METHODS

### Pulse Tubes Design

Two pulse tubes were designed for this study. The first one, used as a reference, is similar to the one used in previous papers [6, 7]. The second is reduced in size, and more particularly in sections, as specified in Table 1. The hot regenerator is considered between the warm interface and intercept 1, and the cold regenerator between intercept 1 and the cold end. The first intercept is an integrated heat exchanger and intercept 2 is a movable ring whose position is fixed in all the presented tests. Regenerator mesh is similar in both pulse tubes: composed of stainless steel screens.

### Experimental setup

In order to measure and understand the pulse tube's performance, two test benches were set up: a cryostat integrating heat flowmeters to obtain the cold power available and the heat flows at in-tercepts, and a pressure drop test bench.

**Table 1.** Pulse tubes size reduction

| | Hot regenerator section | Cold regenerator section | Pulse tube section |
|---|---|---|---|
| Reference pulse tube | 426 mm² | 201 mm² | 48 mm² |
| Miniaturized pulse tube | 235 mm² | 111 mm² | 26 mm² |
| Reduction | 45 % | 45 % | 45 % |

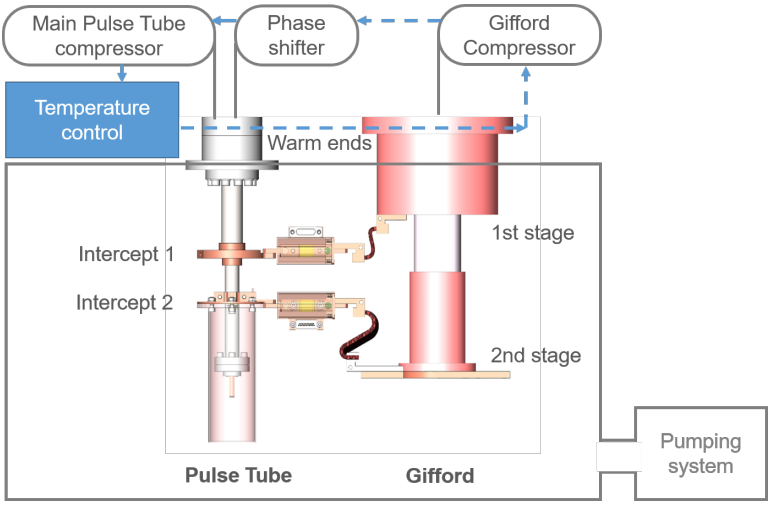


**Figure 2.** Design of the performance cryostat

**Cryostat.** The cryostat is composed of a stainless steel vacuum chamber, actively pumped by a primary and a secondary pump. The warm interfaces of both the Gifford and the pulse tube are regulated with a temperature controller. Three compressors are needed: one is the main compressor of the pulse tube; the second is used as a phase shifter for the pulse tube; and the third one operates the Gifford-McMahon precooler. Suitable heaters and thermometers are positioned at every place of interest. The pulse tube is filled with 21 bars of helium at ambient temperature. To limit the radiation, a thermal screen is attached to the second intercept of the pulse tube, and each element inside the cryostat is wrapped in 10 layers of MLI.

This setup gives us access to the pulse tube performance, the temperatures at interfaces, and the cold power available. It is also used to measure the parasitic heat load of the pulse tube, representing the total heat load (by radiation, convection or internal conduction) arriving at the cold end, by a method described later.

**Heat flowmeters,** illustrated in Figure 3, have been designed and integrated to the experiment to be able to measure the heat flows at both intercepts. Their principle is based on the law of heat conduction (Fourier's law) through a material, reminded in equation (1), where $Q$ is the heat flow, $S$ and $L$ the section and length of the material, $k$ its thermal conductivity and $T_{hot}$ and $T_{cold}$ the temperatures at the ends. After a necessary calibration of the heat flowmeter, knowing the $\Delta T = T_{hot} - T_{cold}$ allows the calculation of heat flow. In our case, the central piece of the heat flowmeter is composed of brass

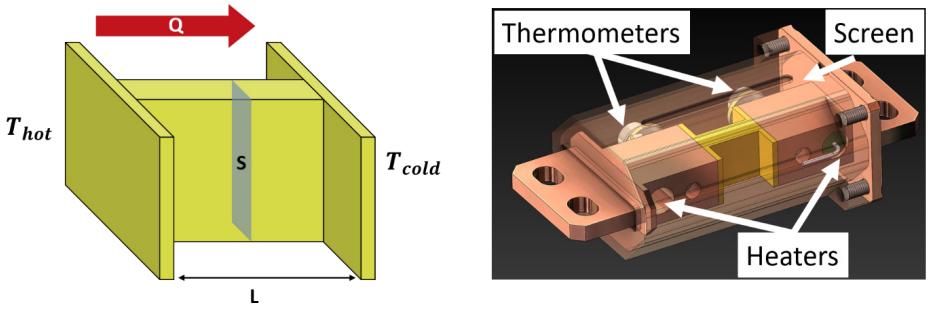


**Figure 3.** Central piece of the heat flowmeter (left) and 3D-view of the assembly (right)

to fit the expected heat flows, and shows a H-shape to increase the interfaces contact surfaces. A thermal screen is added, linked to the cold side of the heat flowmeter to limit the radiation on the bar.

$$Q = \frac{S}{L}\int_{T_{cold}}^{T_{hot}} k(T)dT \tag{1}$$

**Pressure drop test bench.** To measure the pressure drop between the input and output of the pulse tube, the cryocooler is placed inside a test bench where a helium circulation is installed. A set of valves allows regulating the flow through the pulse tube. Suitable pressure sensors and mass flowmeters are used to plot the pressure drop as a function of flow rate, and then obtain a pressure drop coefficient. These measurements are made with continuous flow at ambient temperature, because it has been proven that the evolution of the pressure drop coefficient as a function of the Reynolds number is the same in continuous flow and in oscillating regime [8]. Even if this steady state flow is not fully representative of the real conditions inside the pulse tube cooler, it is then relevant to compare both configurations.

## RESULTS AND DISCUSSION

The same measurements are made on both pulse tubes, the reference and the miniaturized. Pressure drop along the pulse tube, parasitic heat loads on the cold end, performance in terms of achievable temperatures and available cold power, and heat flows at the intercepts are compared and analyzed.

### Pressure drop

The pressure drop between the inlet and outlet of the systems is measured with the test bench previously presented. Figure 4 shows this pressure drop as a function of the helium gas flow through the system for both pulse tubes. An increase of the pressure drop is observed with the flow rate, and the pressure drop is higher in the miniaturized pulse tube than in the reference one.

These observations can be explained thanks to the Darcy-Weisbach equation (2), linking the pressure drop $\Delta P$ to the flow rate $Q$, the density $\rho$, the system length $H$, its section $S$, the hydraulic diameter $Dh$ and the pressure drop coefficient $\Psi$.

$$\Delta P = \frac{\rho Q^2 H}{2S^2 D_h}\psi \tag{2}$$

In a regenerator, this pressure drop coefficient has been estimated to be inversely proportional to the Reynolds number for low Reynolds [9, 10]. These results are translated in equation (3) where $C$ is a constant, $\eta$ the dynamic viscosity and $p$ the regenerator porosity.

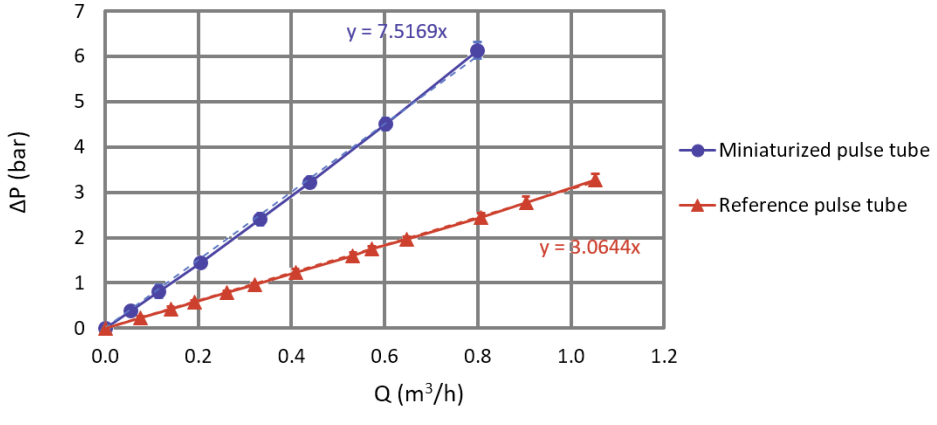


**Figure 4.** Pressure drop as a function of the flow rate for both pulse tubes.

$$\psi = \frac{C}{Re} = C.\frac{pS\eta}{D_h Q\rho} \tag{3}$$

In our case, calculations show a maximum Reynolds number of 10, validating the use of equation (3). The pressure drop can then be expressed by equation (4) where $C_2$ is a new constant. This equation explains the linear increase of the pressure drop as a function of the flow rate observed in Figure 4.

$$\Delta P = C_2.\frac{pH\eta}{SD_h^2}Q \tag{4}$$

To understand the difference in behavior between both pulse tubes, each term of equation (4) can be compared. As their mesh filling is identical, the reference and the miniaturized pulse tubes have the same regenerator porosity. The hydraulic diameter depending only on mesh properties [11], it is constant. By design, both pulse tube have the same length; and the dynamic viscosity is independent of the system geometry. The only parameter that changes is the section so, theoretically, the ratio of pressure drop is described by equation (5).

$$\frac{\Delta P_{miniaturized}}{\Delta P_{reference}} = \frac{S_{reference}}{S_{miniaturized}} \tag{5}$$

When the sections are reduced by 45%, the pressure drop ratio should be equal to 1.82. Actually, Figure 4 shows a higher pressure drop in the miniaturized pulse tube, but with a ratio of 2.45 compared to the reference. Local hydraulic effects may affect the gas flowing through the miniaturized pulse tube, increasing the pressure drop.

Taking into account this increase of pressure drop, the miniaturization of the pulse tube could have a negative effect on the performance.

**Parasitic heat load at cold end**

If the pulse tubes are mounted with redundancy in a cryogenic system for space missions, the parasitic heat load becomes an important problem. Indeed, the OFF heat load of a pulse tube is directly affecting the cold performance of the redundant one in ON state, bringing heat and limiting the cold power available at the cold tip.

Experimentally, these losses are measured using a “PV power decreasing method”, based on an extrapolation of performance with zero compressor input power given to the cold finger. This method is described more precisely in [12] and [13]. It has been internally proven than these measurements are independent of the compressor properties (input power or frequency), which is coherent with the definition of the parasitic heat load.

To complete this study, calculations have been made taking into account the radiation and the conduction. For the radiation, an emissivity of 0.1 has been considered for all surfaces. About the conduction, a conductivity degradation factor of 10% has been chosen through the mesh [14, 15]. Convection is not included in the calculations because external convection is supposed to be negligible thanks to the vacuum environment, and internal convection is difficult to estimate in oscillating conditions.

With the cold end stabilized at 15 K, results are presented in Figure 5 as a function of the intercepts temperatures. When studying the intercept 2 temperature influence, intercept 1 is held at 100 K; and when looking at the intercept 1 temperature, intercept 2 is maintained at 50 K.

Experimentally as numerically, less parasitic heat load is visible in the miniaturized pulse tube compared to the reference one. This result is coherent with the reduction of the sections, bringing less conduction to the cold end. In this sense, the miniaturization of the pulse tube should have a positive effect on the performance.

Moreover, the temperature of intercept 1 has a limited impact on the heat load. On contrary, the important parameter that influences the heat load is the intercept 2 temperature. This result is logical because the conduction on the cold end is mainly driven by its nearest temperature, which is the one of intercept 2. Radiation effects also intervene, as the thermal screen around the cold end in linked to the intercept 2, as seen in Figure 2.

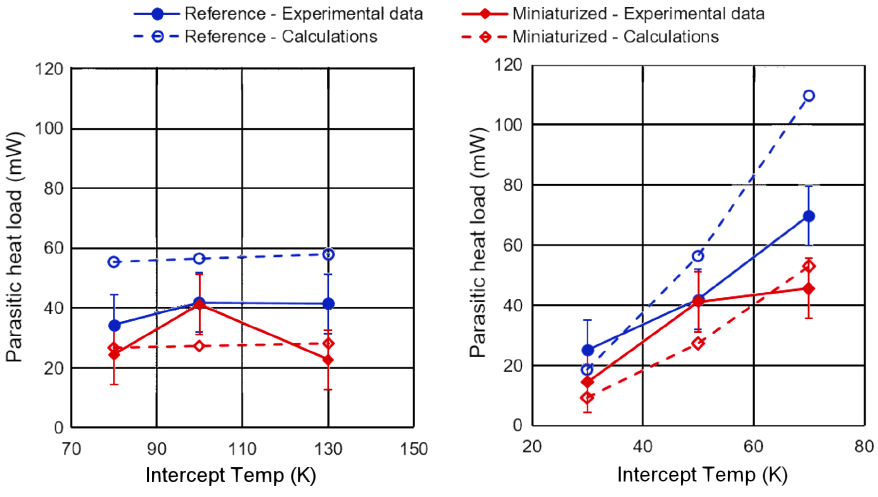


**Figure 5.** Parasitic heat load measurements and calculations

## Cryogenic Performance

Three cryogenic performance parameters were evaluated: the lowest achievable temperature, meaning the cold end temperature with zero cold power; the available cold power at 15 K, considered to be equal to the heating needed to be applied to the cold end to stabilize it at 15 K; and the temperature of the cold end when a heating of 1 W is applied.

The performance was measured for different compressor frequencies (36, 41 or 46 Hz) and compressor powers (50 or 100 W PV). Intercept temperatures were varied from 80 to 130 K for intercept 1, and from 30 to 70 K for intercept 2. For each measurement, the amplitude and voltage of the phase shifting was optimized to obtain the best performance. An example of the comparison of both pulse tube's available cold power as a function of the cold end temperature is presented in Figure 6. To simplify the understanding, this example is shown for a fixed intercept temperatures (100 K for intercept 1 and 50 K for intercept 2) and compressor frequency (41 Hz).

It appears that when decreasing the pulse tube sections, the lower temperature improves, the cold power available at 15 K decreases, and the temperature at 1 W increases.

To study in a comprehensive manner the influence of each parameter, the performance ratios are illustrated in Figure 7. These ratios are defined differently depending on whether they are temperatures or powers, as specified in equations (6), to show a ratio higher than 100% if the miniatur-

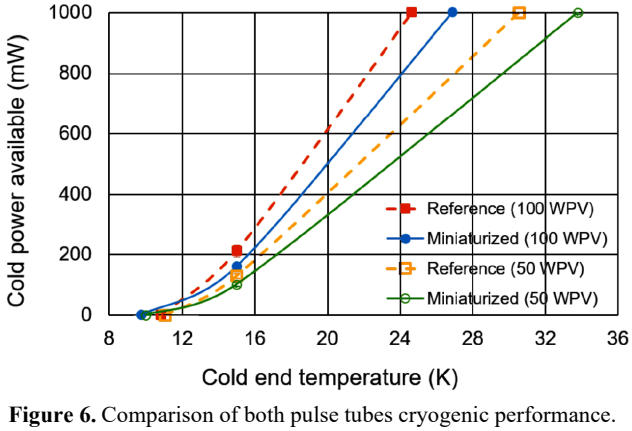


**Figure 6.** Comparison of both pulse tubes cryogenic performance.
(Conditions: 41 Hz, intercept 1 temperature = 100 K, intercept 2 temperature = 50 K)

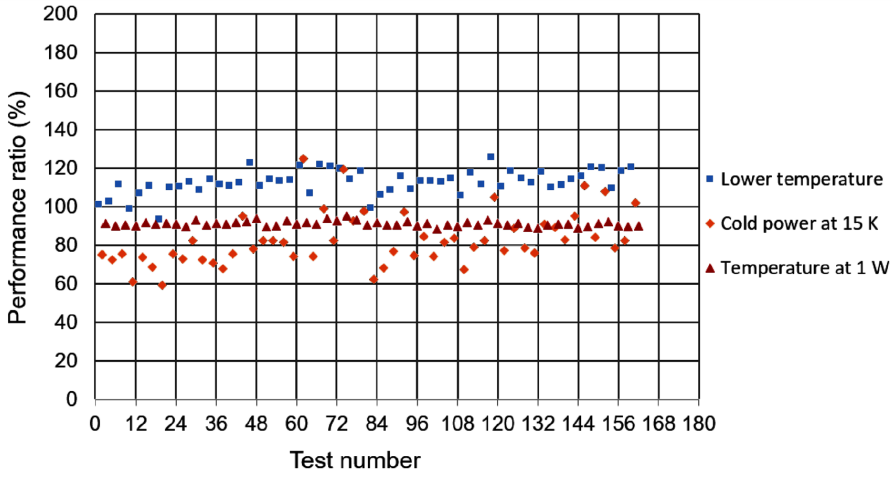


**Figure 7.** Performance ratio between the miniaturized pulse tube and the reference one

ized pulse tube is better than the reference one. Results are presented as a function of test number, the total number of tests being 162 (3 compressor frequencies x 2 compressor input power x 3 intercept-1 temperatures x 3 intercept-2 temperatures x 3 cold end temperatures).

$$P_{Ratio} = \frac{P\,(Miniaturized)}{P\,(Reference)} \cdot 100 \quad \text{and} \quad Ratio = \frac{T\,(Reference)}{T\,(Miniaturized)} \cdot 100 \tag{6}$$

The measurements show that the lower temperature is increased by around 13 % (± 6%) when reducing the pulse tube dimensions. About the cold power available at 15 K, results are more dispersed, but a global decrease of 17 % (± 13 %) was observed with the miniaturized pulse tube. The temperature when the cold end is heated with 1 W is also degraded by 9 % (± 1%) in the small pulse tube.

These observations join the ones previously made in Figure 6. No dependence on any particular parameter could be demonstrated. When reducing the pulse tube sections, the regenerator mass decreases and so does its total thermal capacity. Therefore, it was expected that the miniaturized pulse tube would have a lower performance than the reference one. However, the performance ratios are not trivially related to the reduction of the pulse tube cross-sectional area by 45 %. In addition, the opposite result on the improved temperature limit with the thin pulse tube could be linked to the decrease of the parasitic heat load in this configuration.

### Heat at Intercepts

To check the compatibility of the pulse tubes with a space two-stage pre-cooling, heat flows at intercepts must be quantified. A typical result of the heat flows evolution when changing the pulse tube geometry is presented in Figure 8 with a compressor power of 100 W PV on the left and 50 W PV on the right, under particular conditions: frequency of 41 Hz and temperatures of 100 K at intercept 1 and 50 K at intercept 2.

Measurements show that intercept 1 heat flows are higher than intercept 2 heat flows, which is consistent with their respective temperatures. Heat flows are also more important when the compressor is driven at 100 W PV than at 50 W PV. This behavior is understandable because the gas flow is increasing with the compressor power, requiring more heat flow at the intercepts to be cooled.

Moreover, the existence of a minimum heat flow (at around 15 K) is observed. This trend could be explained by a competition between two effects: when the cold end temperature increases, the temperatures at the intercepts move away from the theoretical gradient, increasing the intercepts heat flows. On the contrary, when the temperature of the cold end cools, it is likely that the increase in heat flows comes from the increase in flow rates at the intercepts.

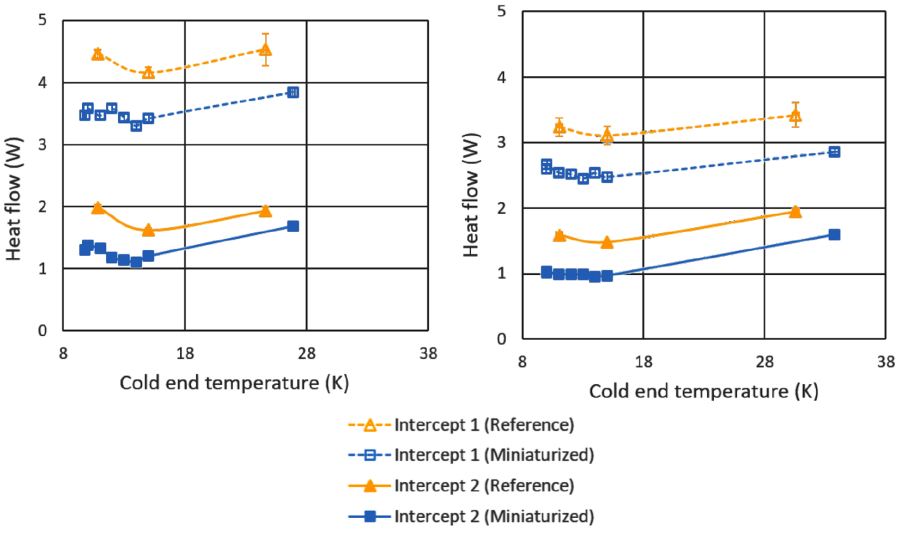


**Figure 8.** Comparison of both pulse tubes heat flows. Left graph: 100 W PV and Right graph: 50 W PV (Conditions: 41 Hz, intercept 1 temperature = 100 K, intercept 2 temperature = 50 K)

**Table 2.** Influence of the miniaturization on the heat flows at intercept.

| **Heat flow ratio** (Miniaturized / Reference) | 50 W PV | 100 W PV |
|---|---|---|
| **Intercept 1** | 84 % (± 11 %) | 83 % (± 7 %) |
| **Intercept 2** | 72 % (± 7 %) | 72 % (± 9 %) |

About the miniaturization, it leads to a decrease of the heat flows on both intercepts. To study more precisely these points, heat flow ratios are quantified in Table 2.

From the data in Table 2, the compressor power seems not to be the important parameter to take into account. Actually, for intercept 2, the heat flow ratio was similar in each case and no significant parameter could have been highlighted. For intercept 1, a trend emerges as a function of its tem-perature: the ratio increases with the temperature, corresponding to the heat flow of the miniatur-ized pulse tube approaching the reference one. In practice, this means that the heat flow gain of the miniaturization is more pronounced when lowering the intercept 1 temperature.

On average, the heat flows are reduced by 16.5 % (± 9 %) for intercept 1 and 28 % (± 8 %) for intercept 2 compared to the reference. This behavior was expected given the sections, and therefore the volumes, which are decreasing. It is still interesting to note that the ratio is, on one hand, differ-ent for both intercepts; and in the other hand, not linear with the sections shrinkage.

## CONCLUSION

This work is based on the idea to achieve a space pulse tube type cooler working under 10 K, which could be compatible with a two-stage space cooler and then providing three temperatures stages. The chosen design is based on a single-stage pulse tube with two intercepts, a configuration that has already proven itself in terms of performance, but requires too much heat flow at the interfaces to be directly compatible.

In order to decrease these heat flows, two pulse tubes have been studied: the reference one, whose performance is known and validated for space applications, and a miniaturized one, whose sections are reduced by 45 %.

Pressure drop measurements have shown an increase of this parameter when miniaturizing the pulse tube, inversely proportional to the sections as expected with calculations. Parasitic heat load

experiments are in agreement with numerical estimations, highlighting a decrease of the heat load at the cold end in the thin pulse tube. Their parameters allow a better understanding of the cryogenic performance results.

Indeed, a reduction of the pulse tube sections of 45 % leads to a decrease of the cold power available at 15 K (- 17 % ± 14 %) and of the temperature when heated at 1 W (- 9 % ± 1 %), which is coherent with a regenerator having less total thermal capacity. On the other hand, the lower temperature is improved by 13 % (± 6%) is the small pulse tube, which is interesting in order to go down to low temperatures.

Heat flows have been quantified, showing a decrease of the heat flows in the miniaturized pulse tube compared to the reference one. This effect is more visible on the intercept 2, whose heat flow is reduced by around 28 % (± 8 %), against 16.5 % (± 9 %) for intercept 1. As the global heat flow reduction is more marked than the performance decrease, this behavior is interesting for our application: it is possible to adjust the heat flow to make it compatible with a two-stage precooler without losing performance.

In particular conditions of the intercept's temperatures, we observed that the miniaturized pulse tube could already be coupled to such a precooler. This new geometry shows advantages in redundant-cooler configurations. However, optimization will be required to obtain the best performance. Now that this first proof of concept is validated, two next steps are planned. A first one is to optimize the whole pulse tube geometry, and not only the sections. Then, a second study of the regenerator composition is planned in order to achieve lower temperatures when keeping a reasonable heat flow at the intercepts.

## ACKNOWLEDGMENT

This work is being conducted with a partial support of CNES. The experimental work at CEA/SBT has been shared by René-Laurent Clerc and Nicolas Besson whose contribution to this project was greatly appreciated.

## REFERENCES

1. Charrier, A., "Pulse tube cryocooler for space applications working at low temperatures (4K-10K)," *Ph.D. of Grenoble Alpes University* (2015).
2. Prouvé, T., Duval, J.M., Charles, I., Martin, S. and Daniel, C., "Demonstration of a 3-Stage Pulse Tube Cooler for Space Applications," *Cryocoolers 20*, ICC Press, Boulder, CO (2019), pp. 17-26.
3. Charles, I., Golanski, L., Gauthier, A., Coynel, A., & Duval, J. M. "20 K coaxial pulse tube using pas-sive precooling," *AIP Conference Proceedings* (Vol. 985, No. 1). American Institute of Physics, (March, 2008), pp. 887-894.
4. Tanchon, J., Trollier, T., Triqueneaux, S., & Ravex, A, "20–50 K and 40–80 K pulse tube coolers: Two candidates for a low temperature cooling chain," *Cryogenics*, 50(1), (2010), pp. 55-60.
5. Charrier, A., Charles, I., Rousset, B., Duval, J. M., & Daniel, C, "Low temperature high frequency coaxial pulse tube for space application," *AIP Conference Proceedings* (Vol. 1573, No. 1, (January, 2014, ). pp. 1010-1017).
6. Duval, J. M., I. Charles, J. Butterworth, J. Mullié, and M. Linder. "7K-15K pulse tube cooler for space," *Cryocoolers 17* (2013), ICC Press, Boulder, CO, pp. 17-23.
7. Pennec, Y., J. Butterworth, G. Coleiro, P. Barbier, S. Martin, P. Crespi, I. Charles, et al., "Engineering model of a high power low temperature pulse tube cryocooler for space application," *Cryocoolers 19*, ICC Press, Boulder, CO (2017), pp. 43-48.
8. Prouvé, T., and Charles, I., "Study of the pressure losses in oscillating regime," *CEA-DSBT Master Thesis* (2002).
9. Tanaka, M., Yamashita, I. and Chisaka, F., "Flow and heat transfer characteristics of the Stirling engine regenerator in an oscillating flow," *JSME international journal. Ser. 2, Fluids engineering, heat transfer, power, combustion, thermophysical properties*, 33(2), 1990, pp. 283-289.

10. Kays, W.M. and London, A.L., *Compact Heat Exchangers*, McGraw Hill (1984).

11. Zhao, Z., Peles, Y. and Jensen, M.K., "Properties of plain weave metallic wire mesh screens," *Interna-tional Journal of Heat and Mass Transfer*, 57(2), 2013, pp. 690-697.

12. Dherbécourt, D., Martin, S., Charles, I., Duval, J.M., André, J. and Daniel, C., "Impact of the cold regenerator mesh geometry on low temperature pulse tube cold finger performance," *IOP Conference Series: Materials Science and Engineering* (Vol. 755, No. 1, p. 012013). March, 2020.

13. Prouvé, T., and Charles, I., "Pulse tube redundancy and parasitic heat losses estimation," *26th Space Cryogenic Workshop* (2015).

14. Kuriyama, T., Kuriyama, F., Lewis, M.A., and Radebaugh, R., "Measurement of Heat Conduction Through Stacked Screens", *Cryocoolers 9*, Springer, Boston, MA (1997), pp. 459-464.

15. Lewis, M.A. and Radebaugh, R., "Measurement of heat conduction through bonded regenerator matrix materials," *Cryocoolers 12*, Springer, Boston, MA (2003), pp. 517-522.